JOURNAL OF CATALYSIS 129, 195–201 (1991)

Surface Area Determination of Supported Oxides: WO_3/Al_2O_3

R. L. BRADY, D. SOUTHMAYD, C. CONTESCU,[1] R. ZHANG,[2] AND J. A. SCHWARZ[3]

Department of Chemical Engineering and Materials Science, Syracuse University, Syracuse, New York 13244-1190

Received July 26, 1990; revised October 30, 1990

The concept that the variation in the point of zero charge (pzc) of physical mixtures of pure oxides can serve as a "calibration curve" to evaluate the surface areas of the individual phases of composite oxides is now applied to the WO_3/Al_2O_3 system. The results of the previously reported model, which assumes the surface area of each component in a composite oxide is a surface area weighted sum of the pzc's of the pure components, are compared to another model that accounts for variations in the measured BET area due to the increased loading of the second phase. The parameters of the models are the number of dispersed clusters and their size, and results from both models show the same qualitative trends. They become quantitatively the same as the second-phase loading decreases. © 1991 Academic Press, Inc.

INTRODUCTION

Surface modification of bulk oxides by attaching other oxides in the form of surface cluster compounds is one way to vary the interfacial properties of the bulk oxide. Cluster compounds of metal oxides can be prepared by aqueous or non-aqueous impregnation of the support oxide, followed by controlled oxidation or other fixing procedures. Recently Connell and Dumesic reported on the properties of a series of binary oxides formed by the drop addition of a metal oxide precursor, at *low* concentration, onto the surface of a second supporting metal oxide (*1–3*). When the second-phase oxide "wets" the support, cluster compounds are formed and the resulting material is referred to as a composite oxide.

Tungsten oxide on alumina is a composite oxide that has been studied by a number of surface science techniques. Below monolayer coverages, Raman spectroscopy results indicate that the tungsten oxide is present as a highly dispersed surface phase bound strongly to the support surface (*4–6*). Salvati *et al.* (*5*) proposed that WO_x species exist as tetrahedral WO_4^{-2}. This structural type was confirmed by X-ray absorption near edge spectroscopy, although there the authors suggest the surface tungsten oxide exists as a distorted tetrahedra (*7*). The surface density of tungsten oxide on alumina at maximum coverage, reported by Vermaire and Van Berge, is 6 WO_3 molecules/nm^2 (*8*). This density points to a stoichiometry of 1 : 2 tungsten oxide molecules per hydroxyl group on the alumina.

Although tungsten oxide exhibits excellent acidic properties, the oxide has a relatively low surface area. Supporting tungsten oxide on a second high surface area carrier yields a class of supports which offer utility in designing supported metal catalysts with unique properties. This design strategy focuses on the idea that adsorption of ionic solutes containing catalytic metals is controlled by surface charge (*9*). This is true only when the ionic solute does not hydrolyze to form hydroxo complexes in solution or interacts with the surface through

[1] Present address: Institute of Physical Chemistry, Spl. Independentei, 202, Bucharest, Romania.

[2] Scientific Committee of Lanzhou, China.

[3] To whom correspondence should be addressed.

0021-9517/91 $3.00

any non-electrostatic bonds. When these conditions are met, selective metal support exchange can be realized by exploiting the surface charge development of oxides during wet impregnation of catalytic precursors. By proper adjustment of the pH of the impregnant, the solid phases of a composite oxide would selectively exchange anionic or cationic catalytic precursors. Before this hypothesis can be tested, it is necessary to determine the pH-dependent surface charge development of this oxide system. In addition, some knowledge of the "structure" of the dispersed phase is desirable, in particular, its surface area.

In a recent study the surface chemistry of TiO_2/Al_2O_3 composites in contact with water has been examined (*10*). It was proposed that the variation in the point of zero charge (pzc) of physical mixtures of the pure oxides could serve as a "calibration curve" to evaluate the surface area of the individual phases of composite oxides. In that work the concentration of the second phase was less than 15% by weight because of solubility limitations of the reagents used. The procedures used to characterize the TiO_2/Al_2O_3 system are extended, herein, to a series of WO_3/Al_2O_3 supports where the second-phase concentration is as high as 30% by weight. Such a high concentration of second-phase oxide could lead to a suppression in the BET area of the supporting oxide. Indeed, we find this to be the case. Consequently, two models for determining the surface areas of the composite oxide phases are proposed. In both cases the physical mixture data are used to establish a calibration curve for assessing the surface areas of the individual oxides in the composites. The first model is a direct extension of the earlier work (*10*); the second model considers the measured BET areas of the composites to be apportioned to each phase on the bases of their pzc and the calibration curve. We find that a qualitative picture of the morphology of the second phase is independent of the model.

EXPERIMENTAL

MATERIALS

A. Pure Supports

(*1*) *Alumina.* The aluminum oxide support material used in this study is a $\frac{1}{16}$-in. extrudate gamma phase supplied by American Cyanamid (Lot No. 85-NA-1402). Its pore volume is 0.484 cm^3/g. The extrudate was ground to 40–80 mesh (particle size ~0.225 mm). Prior to use, the Al_2O_3 was activated by calcining in air at 873 K for 24 h. Its N_2 BET area after calcination is ~153 m^2/g. The calcined oxide was then sealed and stored in glass containers.

(*2*) *Tungsten oxide.* The tungsten oxide support was an Alfa Products (Lot No. B021) 99.7% tungsten (VI) oxide. The tungsten oxide is a non-porous yellow powder with a N_2 BET area of ~1 m^2/g (*11*). Because the WO_3 is non-porous, the pore volume of the powder is assumed to be negligible. The manufacturer reports the size of the powder to be ~320 mesh, which corresponds to particles smaller than 0.044 mm diameter. The WO_3 was calcined at 873 K for 24 h for activation and stored prior to use.

B. Physical Mixtures

Physical mixtures of the two oxides were prepared in the range of 1 to 50% by weight of Al_2O_3. To reduce sampling errors aliquots of the desired mass ratio were prepared individually.

C. Composite Oxides

(*1*) *Tungsten oxide on alumina.* The tungsten oxide precursor was ammonium metatungstate (AMT), molecular weight 2959 g/gmol and molecular formula $(NH_4)_6\ H_2\ W_{12}\ O_{40} \cdot x\ H_2O$ supplied by GTE Sylvania. The degree of hydration of the AMT used was $x = 5$, which results in an equivalent weight of tungsten oxide of 0.913 WO_3/g AMT. The solubility of the AMT is high (1.6 kg/liter) which allowed high weight loadings of WO_3 on Al_2O_3 to be made. Desired weight loadings were achieved by impregnation

with AMT solutions using an amount equivalent to the pore volume of the Al_2O_3. The impregnated oxide was dried at 393 K for 1 h and then calcined at 873 K for 24 h. Composites of 1 to 30% by weight of tungsten oxide were prepared and their BET surface areas were determined after the calcination step. The BET area of the highest weight loading of WO_3 on Al_2O_3 (30%) is 109 m^2/g. The relative error in all BET measurements is estimated to be less than 5% for samples with surface area greater than 100 m^2/g.

Impregnation solutions corresponding to the highest and lowest loadings of WO_3 were prepared for further characterizations. Two drops of AMT solution (containing, respectively, 7.71 and 0.56 g AMT in 10 cm^3 water) were evaporated at 343 K on a glass slide and the crystals formed observed using an optical microscope (Nikon 52761) at 220× magnification.

(*2*) *Aluminium oxide on tungsten oxide.* To prepare alumina on tungsten oxide supports, aluminum isopropoxide (Aldrich Chemicals, lot No. 05228AT) was dissolved in a desired amount of toluene. The amount of solution used to wet a known weight of WO_3 was determined by successive trials to be 0.125 cm^3/g and appropriate weights of WO_3 were used to achieve desired weight loadings of alumina on tungsten oxide. Preparation was carried out in a N_2 purged glove box; the composites were then dried at room temperature for 1 h and calcined at 873 K for 24 h. The solubility of aluminum isopropoxide limits the Al_2O_3 weight loading to less than 10%. The BET areas of these composites are not reported because the relative error of the measurement exceeds the absolute values of the individual areas.

PROCEDURES

The pzc's of all the oxides were determined by mass titration (*12*), which involves finding the asymptotic value of the pH of an oxide/water slurry as the oxide mass content is increased. Varying amounts of oxide/water ratios by weight (0.1 to 60%) were allowed to equilibrate in distilled water for 24 h. A Fisher Accumet pH meter, model 805MP,and a Corning pH meter, model 145, were used to measure the pH of the equilibrated solutions. Both meters were calibrated with pH 4 and pH 10 certified buffer solutions supplied by Fisher Scientific Company. A Debye–Scherrer X-ray powder camera was used for X-ray diffraction studies. The powder samples were mounted on an optical coated fiber, centered in the rotating sample holder and irradiated with nickel filtered Cu$K\alpha$ radiation (1.542 Å) for approximately 45 min. A Kodak direct exposure film was used in all these studies. The two pure oxides and selected composites were studied.

RESULTS

Figure 1 shows typical plots of pH versus mass percentage of oxide for the pure supports and selected physical mixtures. The plateaus of the mass titration curves correspond to the pzc's of the oxides (*12*). Values of 8.5 ± 0.05 and 4.0 ± 0.05 are found for Al_2O_3 and WO_3, respectively. These are in agreement with values reported in the literature. The accuracy of the pH measurement depends on the calibration of the pH meter, which in our case corresponds to ±0.05 pH units.

Table 1 shows the pzc's for a range of physical mixture compositions. Also shown are the weight fraction of WO_3 and the area fractions of both WO_3 and Al_2O_3. A BET area of 153 m^2/g for alumina was used in the calculation of the results presented in Table 1. Any error in determination of the low BET area of WO_3 contributes a certain amount of error to the values in Table 1. Our measurement indicates a N_2 area of 1.5 m^2/g while that determined by Murrell is 1 m^2/g (*11*). SEM analysis showed, from 110 measured particle sizes and assuming a hard sphere approximation, the surface area to be 0.2 m^2/g. A value of 1 m^2/g was used for convenience to calculate the area fractions

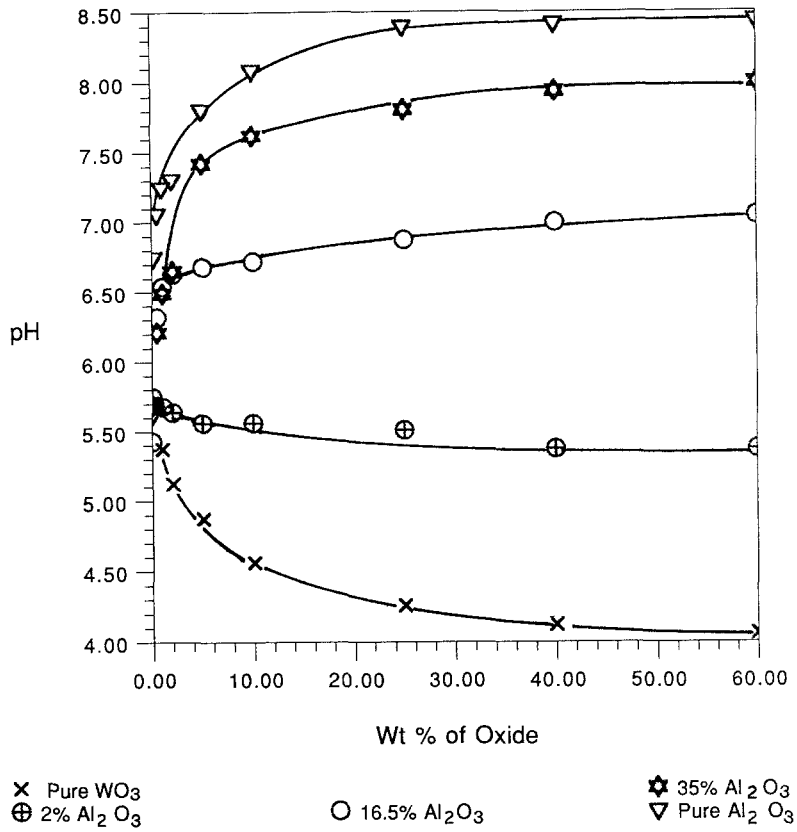

FIG. 1. Plot of pH versus oxide/water mass percentage for alumina, tungsten oxide, and various physical mixtures of alumina and tungsten oxide. Mass fractions are given in legend. The estimated error in the measurement is comparable to the size of the symbols. The lines drawn connecting the data are for clarity.

given in Table 1. An error of ±25% in this value results in less than ±10% error in the evaluation of surface area. The results presented in Table 1 demonstrate that the physical mixtures have pzc values between the values for the pure supports.

Table 2 presents the pzc values for both sets of composite oxides and the corresponding values of the weight loadings of the second phase. The composite oxides have pzc's between those of the pure oxides. At a concentration of 30% WO_3 on Al_2O_3, the pzc is nearly that of bulk WO_3.

From previous work done on the TiO_2/Al_2O_3 system it was suggested that the data presented in Tables 1 and 2 could be used, in conjunction with a model for the structure of the dispersed phase, to evaluate the surface area of supported oxides (*10*). The intermediate step in extending this earlier analysis to the WO_3/Al_2O_3 system is establishing a calibration curve (based on BET areas of pure components) which relates the pzc of the physical mixtures to the area fraction contributed by tungsten oxide. For mathematical convenience, the physical mixture data were fit to the equation

$$Y = A + B \cdot X^C, \qquad (1)$$

where Y = area fraction contributed by WO_3 and X = pzc of physical mixture. The values of A, B, and C were determined by non-linear regression and found to be $A = -0.026$; $B = 1160.1$; $C = -5.0$ with corre-

TABLE 1

Summary of Results for Physical Mixtures: pzc, Weight Fraction of Tungsten Oxide and Area Fraction Contributed by the Pure Components

Weight fraction WO_3	Area fraction WO_3	Area fraction alumina	pzc pH Units
1.000	1.0000	0.0000	4.08
0.994	0.5084	0.4916	4.71
0.989	0.3469	0.6531	4.96
0.979	0.2077	0.7923	5.38
0.949	0.0953	0.9047	6.10
0.909	0.0531	0.9469	6.39
0.875	0.0374	0.9626	6.76
0.835	0.0273	0.9727	7.04
0.750	0.0164	0.9836	7.43
0.650	0.0102	0.9898	7.93
0.600	0.0083	0.9917	8.21
0.000	0.0000	1.0000	8.50

lation coefficient = 0.997. The regression line and the physical mixture data are shown in Fig. 2.

DISCUSSION

Assuming the second phase in the composites to be highly dispersed and hemispherically shaped, Subramanian *et al.* (*10*) determined the surface areas of the supported oxides for the TiO_2/Al_2O_3 system.

TABLE 2

Weight Fraction of Second Phase in Composite Oxides, Q, and Corresponding pH_{pzc}: (A) WO_3 on Al_2O_3; (B) Al_2O_3 on WO_3

A. Tungsten oxide on alumina		B. Alumina on tungsten oxide	
Q	pH_{pzc}	Q	pH_{pzc}
0.300	4.24	0.0507	6.03
0.204	5.25	0.0200	5.87
0.150	5.64	0.0075	5.75
0.121	6.08	0.0030	5.60
0.075	6.99	0.0010	5.10
0.050	7.76	0.0008	4.75
0.025	8.14	0.0005	4.10
		0.0003	4.08

Their analysis, designated model 1, is used here to evaluate the surface areas of Al_2O_3 and WO_3 as second phases.

A surface area weight relationship based on the BET areas of the pure phases is used to relate the experimentally measured pzc of the composites to surface areas of each component in the oxide system. The parameters of the model, described in detail elsewhere (*10*), are Q = weight fraction of second phase, N = number of dispersed clusters, d = diameter of the clusters. Values of Q, d, N, and the surface area of the second phase, $[2\pi N(d/2)^2]$, are presented in Table 3.

A second model was considered. In this case the area fraction of the second phase (F) was determined by using the experimentally measured pzc of the composite oxides and the calibration curve derived from the physical mixtures. The model parameters were then calculated from measured total BET areas of the composites (S_{BET}) and the known weight fraction of the second phase. The results of model 2 for the WO_3 on Al_2O_3 composites only are also presented in Table 3. The model parameters agree quite closely at low weight loadings of WO_3 (Table 3 A,B) with the largest deviations occurring for concentrations greater than 15% weight of WO_3. Table 3C shows only the results of model 1 applied to Al_2O_3 on WO_3 because accurate BET surface areas could not be obtained. In light of the agreement between both models at low concentrations of second-phase oxide (Table 3 A,B) we believe the results shown in Table 3C are reliable.

The X-ray diffraction patterns of the composite oxide showed only the characteristic lines of the support. This indicates that the second phase was either not of sufficient size or of sufficient surface cluster density to cause diffraction. Both Al_2O_3 and WO_3 have strong lines that, if present in a large enough particle in the second phase, would be expected to diffract. The absence of diffraction features for the second phase in the X-ray results supports the majority of the values of the calculated diameters. Values

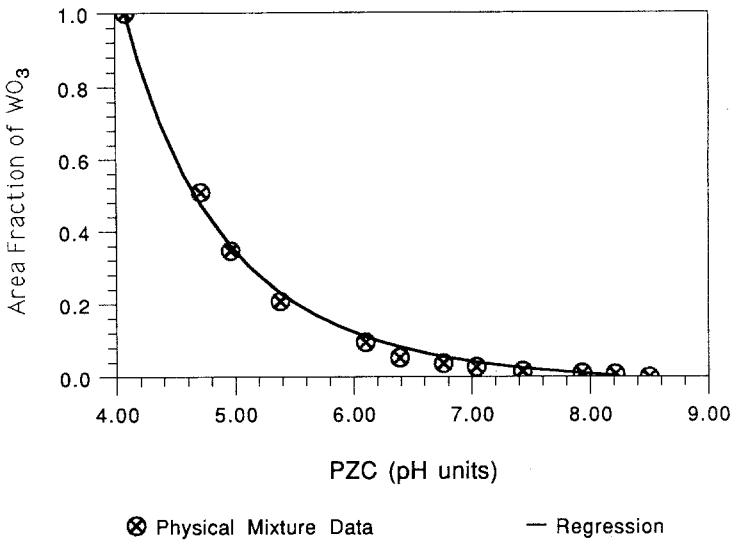

FIG. 2. Area fraction of WO_3 versus pH_{pzc} of physical mixtures. Solid line [Equation (1)] is nonlinear least squares regression line and points are physical mixture data.

of d in excess of 100 Å are accompanied with low values of N, the number of clusters. This could be the reason why no second-phase diffraction features were found.

A striking result obtained from both model calculations is the decrease in the mean diameter of dispersed WO_3 clusters as its weight loading increases. This behavior is opposite to the general trend observed in dispersing a metallic phase in supported catalysts. To understand these observations, the dynamics of the precipitation process of a solid phase within the pores of a supporting oxide must be examined. A macroscopic analog is the crystalline skeleton remaining after drying AMT solutions of different concentrations. Diluted AMT solution (0.056 g/cm^3) yielded long needle-

TABLE 3

Weight Loading of Second Phase in Composite Oxides, Q, and Corresponding Model Parameters: (A) WO_3 on Al_2O_3 (model 1); (B) WO_3 on Al_2O_3 (model 2); (C) Al_2O_3 on WO_3

A				B					C			
Q	N ($\times 10^{-7}$)	d (Å)	S (m^2/g)	S_{BET} (m^2/g)	F	N ($\times 10^{-17}$)	d (Å)	S (m^2/g)	Q	N ($\times 10^{-16}$)	d (Å)	S (m^2/g)
0.03	0.013	216.5	0.96	146	0.006	0.012	221.6	0.94	0.0005	0.0012	374	0.03
0.05	0.045	180.0	2.28	148	0.015	0.042	185.2	2.24	0.0008	13.7	18.7	0.08
0.08	0.50	92.7	6.74	144	0.04	0.341	107.5	6.19	0.001	21.2	17.8	1.05
0.12	3.85	55.1	18.36	130	0.11	1.86	69.9	14.30	0.003	5.25	40.9	1.38
0.15	10.6	42.2	29.60	130	0.18	4.97	54.3	23.02	0.007	0.987	96.8	1.45
0.20	23.1	36.6	48.60	129	0.26	9.18	48.7	34.19	0.020	0.155	249	1.51
0.30	973.8	11.8	213.0	109	0.82	72.5	28.0	89.38	0.051	0.027	605	1.57
									0.079	0.012	926	1.61

Note. N, number of dispersed clusters; d, diameter of clusters; S, surface area of second phase.

shaped cyrstals with a fiber-like appearance. The concentrated AMT solution (0.771 g/cm^3) produced many small spot-like crystals. The following scenario is consistent with the model's parameters and the visual observations of the results of the drying process. A variation in weight loading of second-phase oxide by the incipient wetness procedure is achieved by increasing the concentration of the impregnating solution. The pH's of the most diluted and most concentrated AMT solution are 3.6 and 2.6, respectively. Alumina dissolution and the accompanying introduction of defects in the Al_2O_3 framework occur at these low pH values. In the aqueous phase, the degree of polymerization of the metatungstic acid is controlled by pH, temperature, and solution concentration. The dynamics of drying are such that the higher the concentration of pore filling solution, the faster a state of supersaturation will be reached, leading to a faster nucleation rate, and therefore to a larger number of smaller crystallites. This is confirmed by the macroscopic observations of the results of the drying process. Alumina dissolution continuously provides the template for adsorption sites of the precipitant. The results from both models, along with this scenario, suggest that subsequent calcination of the composite precursor does not destroy the template established during impregnation.

A monolayer coverage of WO_3 on Al_2O_3 would have a pzc identical to pure WO_3 because water molecules would be masked from the Al_2O_3 surface by the WO_3 shell. For a 153 m^2/g Al_2O_3 support, a monolayer coverage of 6 WO_3 molecules/nm^2 (*8*) would correspond to a 26% WO_3 loading. However, the pzc of the 30% WO_3 composite studied here is 4.24, which indicates the existence of exposed Al_2O_3 surface (cf. WO_3, pzc = 4). This is consistent with the model results which show either a total base area of WO_3 clusters $[\pi N(d/2)^2]$ lower than that of initial alumina (model 1) or a 18% contribution of Al_2O_3 surface to the total BET surface of the composite with 30% WO_3 (model 2).

ACKNOWLEDGMENTS

Portions of this work were supported by NSF under Grant CBT-8900514 and U.S. Air Force through Contract No. F30602-89-C-0113. One of us (C.C.) acknowledges support of the IREX board.

REFERENCES

1. Connell, G., and Dumesic, J. A., *J. Catal.* **101,** 103 (1986).
2. Connell, G., and Dumesic, J. A., *J. Catal.* **102,** 216 (1986).
3. Connell, G., and Dumesic, J. A., *J. Catal.* **105,** 285 (1987).
4. Ng, K. T., and Hercules, D. M., *J. Phys. Chem.* **80,** 2094 (1976).
5. Salvati, L., Jr., Makovsky, L. E., Stencel, J. M., Brown, F. R., and Hercules, D. M., *J. Phys. Chem.* **85,** 3700 (1981).
6. Stencel, J. M., Makosky, L. E., Diehl, J. R., and Sarkus, T. A., J. Raman, *Spectrosc. Lett.* **15,** 282 (1984).
7. Horsley, J. A., Wachs, I. E., Brown, J. M., Via, G. H., and Hardcastle, F. D., *J. Phys. Chem.* **91,** 4014 (1987).
8. Vermaire, D. C., and Van Berge, P., *J. Catal.* **116,** 309 (1989).
9. Schwarz, J. A., *in* "AIChE National Meeting, Washington, DC, November 1988."
10. Subramanian, S., Noh, J. S., and Schwarz, J. A., *J. Catal.* **114,** 433 (1988).
11. Murrell, L. L., private communication.
12. Noh, J. S., and Schwarz, J. A., *J. Colloid Interface Sci.* **130,** 157 (1989).